Distribution Statement

Distribution A: Public Release.

The views presented here are those of the author and are not to be construed as official or reflecting the views of the Uniformed Services University of the Health Sciences, the Department of Defense or the U.S. Government.

UNIFORMED SERVICES UNIVERSITY OF THE HEALTH SCIENCES
POSTGRADUATE DENTAL COLLEGE
NAVAL POSTGRADUATE DENTAL SCHOOL
8955 WOOD ROAD
BETHESDA, MARYLAND 20889

THESIS APPROVAL PAGE FOR MASTER OF SCIENCE IN ORAL BIOLOGY

Title of Thesis: Characterization of Titanium Implant Surfaces after Nd:YAG Laser Treatment

Name of Candidate: Alex P. Long
Master of Science Degree
June 01, 2022

THESIS/MANUSCRIPT APPROVED: DATE:

KIM.JEFFREY.J.1553853377 Digitally signed by KIM.JEFFREY.J.1553853377 Date: 2022.06.06 09:52:42 -04'00' 6/6/22

Jeffrey J. Kim
CHAIRMAN, RESEARCH DEPARTMENT, NAVAL POSTGRADUATE DENTAL SCHOOL
Committee Chairperson

WILSON.JOHN.HINTON.1063846941 Digitally signed by WILSON.JOHN.HINTON.1063846941 Date: 2022.06.06 09:27:45 -04'00' 6/6/22

John H. Wilson
CHAIRMAN, PERIODONTICS DEPARTMENT, NAVAL POSTGRADUATE DENTAL SCHOOL
Committee Member

MERCHANT.KEITH.ROSHANALI.1246800444 Digitally signed by MERCHANT.KEITH.ROSHANALI.1246800444 Date: 2022.06.06 09:08:12 -04'00' 6/6/22

Keith R. Merchant
PROGRAM DIRECTOR, PERIODONTICS DEPARTMENT, NAVAL POSTGRADUATE DENTAL SCHOOL
Committee Member

CHARACTERIZATION OF TITANIUM IMPLANT SURFACES AFTER Nd:YAG LASER TREATMENT

by

Alex Preston Long
Lieutenant, Dental Corps
United States Navy

A thesis submitted to the Faculty of the
Periodontics Graduate Program
Naval Postgraduate Dental School
Uniformed Services University of the Health Sciences
In partial fulfillment of the requirements for the degree of
Master of Science
in Oral Biology
June 2022

ACKNOWLEDGMENTS

Several individuals have contributed in many ways to the success of this project. First, to the NPDS Periodontics staff members, CAPT John Wilson and CAPT Keith Merchant. They have provided consistent mentorship throughout project construction, development and carryout. Next, LCDR Allison Weinberg, the initial principle investigator who completed the majority of project design, achieved IRB approval, acquired necessary materials and initiated preliminary testing with accompanying results. Also, many thanks to Dr. Jeffrey Kim, NPDS research mentor who has provided consistent support and feedback throughout the project. As well as Dr. Francois Tuamokumo, who aided in statistical analysis. Lastly, Dr. Dennis McDaniel from USU Microscopy who provided training and guidance necessary for microscopic analysis and Dr. Peter Liacouras from 3D Medical Applications Center who designed and fabricated required components.

DISCLAIMER

The views presented here are those of the author and are not to be construed as official or reflecting the views of the Uniformed Services University of the Health Sciences, the Department of Defense or the U.S. Government.

ABSTRACT

Characterization of Titanium Implant Surfaces after Nd:YAG Laser Treatment

Alex Preston Long, DDS, 2022

Thesis directed by: Jeffrey J. Kim, DDS, PhD,
Chairman, Research Department
Naval Postgraduate Dental School

Current literature lacks sufficient evidence of the potential effects lasers can have on dental implant surface topography. The purpose of this *in vitro* study is to analyze the surface roughness (Ra) alterations to titanium disks following exposure to a neodymium-doped: yttrium, aluminum, and garnet (Nd:YAG) laser at clinically relevant angles (0°, 10°, 20° and 30°) and energy values (90 J). Forty titanium implant test disks were selected with unexposed areas serving as controls. A custom assembly provided proper orientation and standardized energy exposure. Through confocal microscopy, three-dimensional images of each disk were obtained and analyzed using scientific imaging software. A one-way ANOVA revealed no significant differences in surface roughness (Ra) when comparing unexposed control areas to laser exposed areas at all angles tested. No significant surface roughness alterations were found on titanium implant disks following Nd:YAG laser irradiation up to an energy angulation of 30°.

TABLE OF CONTENTS

LIST OF TABLES vi

LIST OF FIGURES vii

LIST OF ABBREVIATONS viii

CHAPTER 1: Introduction 1

Peri-implantitis ..... **Error! Bookmark not defined.**
Lasers and Peri-implantitis Treatment 2
Titanium Imiplant Surface and Laser Treatment 3

CHAPTER 2: Materials and Methods 6

Study Design 6

CHAPTER 3: Results 12

Disk Exposure and Image Analysis ..... 1**Error! Bookmark not defined.**
Visual Appearance ..... 1**Error! Bookmark not defined.**
Surface Topography Analysis ..... 1**Error! Bookmark not defined.**
Surface Roughness Parameters 13

CHAPTER 4: Discussion 16

Comparative Literature Outcomes 16
Potential Clinical Impact 18

CHAPTER 5: Conclusions 20

REFERENCES 21

LIST OF TABLES

Table 1. Descriptive Statistics and Independent t-test 18

Table 2. One-way ANOVA and Surface Roughness Parameters 19

LIST OF FIGURES

Figure 1. Clinical laser angulation scenarios .....**Error! Bookmark not defined.**

Figure 2. Custom jig assembly..... 10

Figure 3. Programmable linear actuator..... 11

Figure 4. Photograph of disk groups..... 14

Figure 5. Plot profile images.....1**Error! Bookmark not defined.**

Figure 6. Surface plot images 16

Figure 7. Computed topography images..... 17

LIST OF ABBREVIATONS

Arithmetic surface roughness – Ra

Analysis of variance – ANOVA

Carbon dioxide – CO_2

Carl Zeiss Imaging Data – CZI

Computer aided design / computer aided manufacturing – CAD/CAM

Erbium-doped: yttrium, aluminum and garnet – Er:YAG

Fiji is just imageJ – FIJI

Neodymium-doped: yttrium, aluminum, and garnet – Nd:YAG

Height difference - Rt

Hertz - Hz

Institutional Review Board – IRB

Joules – J

Light amplification by stimulated emission of radiation - LASER

Laser scanning microscope – LSM

Quadratic average – Rq

Millimeters – mm

Micrometers - μm

Nanometers – nm

Naval Medical Leader and Professional Development Command – NMLPDC

Naval Postgraduate Dental School – NPDS

Walter Reed National Military Medical Center – WRNMMC

Watts – W

CHAPTER 1: Introduction

PERI-IMPLANTITIS

Peri-implantitis is an inflammatory condition around a dental implant resulting in loss of supportive bone.[1] Significant esthetic and functional challenges are likely to present over time if peri-implantitis is left untreated. This pathological state is thought to be preceded by a reversible condition termed peri-implant mucositis, which presents as an inflammatory lesion in the absence of progressive bone loss.[2] Although dental implants are often the treatment of choice for replacement of missing teeth, implants do not come without complications. As dental implants become more and more commonplace, there is a correlated increase in prevalence of peri-implant diseases and conditions. Statistics regarding implant placement have shown to demonstrate consistent and substantial increases in dental implant therapy prevalence since 1999[3]. These prevalence increases are anticipated to continue into the future at a high rate.[3] Alongside this prevalence is a corresponding increase in peri-implant diseases and conditions, demonstrated in a systematic review and meta-analysis showing peri-implant mucositis and peri-implantitis rates of 43% and 22%, respectively.[4] Corrective measures for peri-implant disease have proven to be a challenging endeavor with no universally accepted treatment protocol. A myriad of techniques, protocols, and materials have been reported in the literature with variable results.[5] It has been shown that non-surgical therapy has significant limitations in treating peri-implant disease; however, the use of dental lasers as an alternative non-surgical modality has become more prevalent.[6]

LASERS AND PERI-IMPLANTITIS TREATMENT

LASER stands for light amplification by stimulated emission of radiation, and there are numerous applications for lasers in oral procedures.[7] The first use of lasers in dentistry was reported in 1985, and lasers play an integral role in the dental practices of today.[8] Laser interactions with hard and soft tissues of the oral cavity are based upon the emitted wavelength of the laser type and the nature of the atoms and molecules contained in the exposed tissues. This interaction can produce therapeutic affects in dental and periodontal treatment. A key etiologic component of peri-implant disease is the presence of a peri-implant biofilm and the host's immune response that creates a dysbiotic environment that can promote disease.[1] One purported advantage of dental lasers is the notion that the biofilm and associated pathogenic bacteria on implant surfaces may be reduced through the absorption of laser energy.[9] The diseased soft tissue lining in areas of periodontal breakdown has been shown to be removed by lasers with subsequent clot formation leading to successful regenerative outcomes around teeth.[10] Additional advantages include improved hemostasis control, decreased patient discomfort, and improved esthetic outcomes compared to traditional periodontal surgery modalities.[11, 12]

Many lasers have been utilized in the dental setting including diode lasers, carbon dioxide (CO_2) lasers, erbium-doped: yttrium, aluminum and garnet (Er:YAG) lasers, and neodymium-doped: yttrium, aluminum and garnet (Nd:YAG) lasers. An American Academy of Periodontology best evidence consensus statement reports on limited studies and inconclusive results shown in the literature regarding potential implant surface alterations from laser therapy.[13] Based on the varying properties of different lasers, the effect that laser exposure may have on various host tissues and restorative dental materials could be significant. In an *in vitro* study, several commonly used lasers in

dentistry were shown to detrimentally affect various composite, ceramic, and metal restorative materials, including titanium.[14]

Titanium Implant Surface and Laser Treatment

Many advantages have been demonstrated in terms of implant surface roughness and wound healing. Benefits include increased surface area for hard tissue interaction, heightened cell-to-cell interaction and attachment, and improved bone-to-implant contact leading to enhanced healing outcomes.[15] Microsurface texturing of implants has also shown to increase hydrophilicity of the dental implant surface leading to increased blood approximation to implants surfaces for enhanced healing.[16] Alterations to the surface topography of dental implants may lead to changes in how peri-implant tissues heal following laser therapy.

The Nd:YAG laser has specific characteristics that make it a preferred choice for the treatment of peri-implant conditions. Operating at a wavelength of 1,064 nm, the Nd:YAG is primarily absorbed by pigmented tissues and poorly absorbed by water.[17] This allows for the elimination of pigmented pathogenic bacteria while also assisting in favorable coagulation and oral tissue hemostasis. Despite these favorable qualities, it has been demonstrated that titanium surfaces are visibly altered by exposure to the Nd:YAG laser, manifesting as surface alterations and cracking.[14] Studies have further demonstrated that laser exposure can affect the surface microtexture and roughness of titanium implants, resulting in melting and flattening.[18] Others have reported loss of porosity and microfractures in titanium surfaces following laser exposure, even at the lowest power

setting.[19] Additionally, when exposed, roughened implants have been shown to harbor more biofilm compared to machined or smooth implants.[20]

Although there is not a universally accepted protocol for ideal peri-implant laser therapy, it is advised to refrain from direct laser contact with the implant surface and orient the laser energy parallel to the implant body (Figure 1). Given the variations in implant restoration contour and the often-challenging access to implants in posterior sextants, it can be extremely difficult to adhere to the recommended orientation guidelines. The literature demonstrates significant detrimental effects of direct laser exposure on titanium surfaces; however, there have been limited reports evaluating the influence of the exposure orientation on implant surface alterations. It is hypothesized that an increasing angle of laser irradiation results in decreased surface roughness. Therefore, the purpose of this *in vitro* study is to analyze the alterations to titanium disk surfaces following exposure with an Nd:YAG laser at clinically relevant angles and energy values.

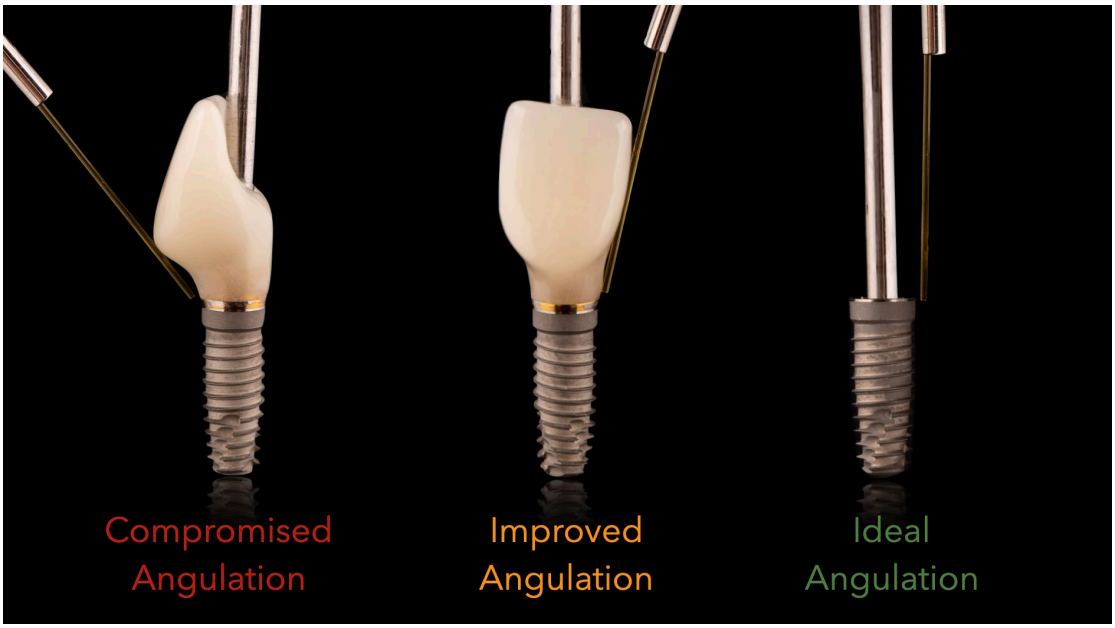

Figure 1. Clinical laser angulation scenarios. Clinical laser angulation scenarios showing compromised, improved, and ideal orientation of laser fiber. As demonstrated in the images, the presence of a crown affixed to the implant impedes the ability to direct the laser energy parallel or away from the implant body.

CHAPTER 2: Materials and Methods

STUDY DESIGN

This study was reviewed by the WRNMMC IRB and declared as research not involving human subjects. The proposed design and study protocol was reviewed and approved by NPDS and NMLPDC, Bethesda, Maryland.

Forty titanium implant test disks were selected based on a sample size power analysis. Disks were 10 mm in diameter, 1 mm in height, and contain a machined surface on one side and roughened surface on the opposing side. Unexposed disk areas served as controls. Disks were provided by Biohorizons® and were fabricated by the manufacturer for implant testing purposes. These titanium disks were designed to mimic commercially available dental implants in terms of metallic composition and surface treatment for enhanced roughness characteristics. The manufacturer utilizes resorbable blast texturing to create a highly irregular surface topography. Disks were randomly assigned to one of four groups based on the clinically relevant angulations of laser irradiation at 0° (disks 1-10), 10° (disks 11-20), 20° (disks 21-30) and 30° (disks 31-40). On the non-tested machined side, engravings were completed on all disks with a number corresponding to the assigned test group. On the tested roughened side, two depressions with a surgical bur were created near the periphery of each disk, indicating the planned area for laser exposure in between the markings across the full diameter of the disks.

Through computer-aided design and computer-aided manufacturing (CAD/CAM) a custom jig assembly was fabricated to position an Nd:YAG laser handpiece (Periolase® MVP-7™, Millennium Dental Technologies, LLC) (Figure 2). The laser's

fiber optic cable was housed in the handpiece and secured in the jig assembly for proper and reliable orientation and energy exposure. Four openings in the assembly served as guide tubes, corresponding to the desired fiber-disk relationship angles being tested (0°, 10°, 20° and 30°). The jig assembly was affixed to the top of a programmable linear actuator (Figure 3).

Linear actuators are machines that convert rotational motion into linear motion. These devices are proven constructs capable of moving loads in a directionally straight manner. The linear actuator selected for this study (CYNOHO®) uses a powered step-wise motor to move an attached base component along a fixed track. A programmable device is connected to the actuator that allows for a set speed and time to run. This setup provided the standardized energy delivery at a consistent angular orientation and repeatable speed. A platform with a corresponding diameter to retain the titanium disks was secured along the actuator's fixed track providing the linear motion desired. Therefore, the laser handpiece and fiber maintained a set position, while the test disks and underlying base move in a horizontal linear fashion.

The Nd:YAG laser delivered a standardized total of 90 J per disk with common settings used in the treatment of peri-implantitis. The Periolase unit was set to ablation mode with the following parameters: 100 μsec, 3.6 W, 20 Hz. The fiber was properly cleaved and tested to ensure 3.6 W delivery and placed in the appropriate position for exposure. Testing for proper energy delivery values was completed prior to each exposure. The tip of the laser fiber was placed 1 mm above each test disk in a standardized fashion using a spacer guide measuring 1 mm in height. The linear actuator was programmed to accelerate the disks at a constant speed while irradiation was

completed over 28 seconds across the full disk diameter indicated between depression markings.

A Zeiss LSM 980 laser scanning confocal microscope was used to capture three-dimensional images of each disk in a standardized fashion. In order to appropriately analyze the images for surface topography, 63x magnification was used to scan the z-dimension of each disk. The test areas selected for imaging were located immediately horizontal to the created depressions near the disk periphery. This was done to ensure the selected disk portion had been irradiated. The initial locations were positioned using a 10x lens prior to image capture with the 63x magnification lens. Control areas were randomly selected in unexposed locations from disks in each test group. In order to properly capture the surface topography of each sample, a stack of images (z-stack) capturing the highest peak and lowest valley was compiled by assigning an image capture range based on pixel density. Hundreds of individual images or slices were contained in the z-stacks, each being 0.05 μm apart from the other. Imaged areas were 135 μm x 135 μm. This method involved manually selecting a scanning range above and below the observable surface to ensure the entire z-dimensional surface was contained within the image data. Once scanning was complete, a CZI (Carl Zeiss Image Data) file was created and used for analysis.

Images were analyzed using a scientific open source Java imaging software, FIJI. The CZI files were imported into the software and calibrated to the known dimensional setting used during image capture. Images were analyzed using the SurfTool 1B plugin and converted to Tag Image File Format (tiff) files.[21] The SurfCharJ 1q plugin was then used to generate the surface characteristic information from each file.[21] Generated data

included the arithmetic average roughness (Ra) which was then used to determine quantitative topographical data of unexposed and laser exposed areas. Further observational analysis was completed using additional FIJI features, such as computed topography, surface plotting, and plot profiling.

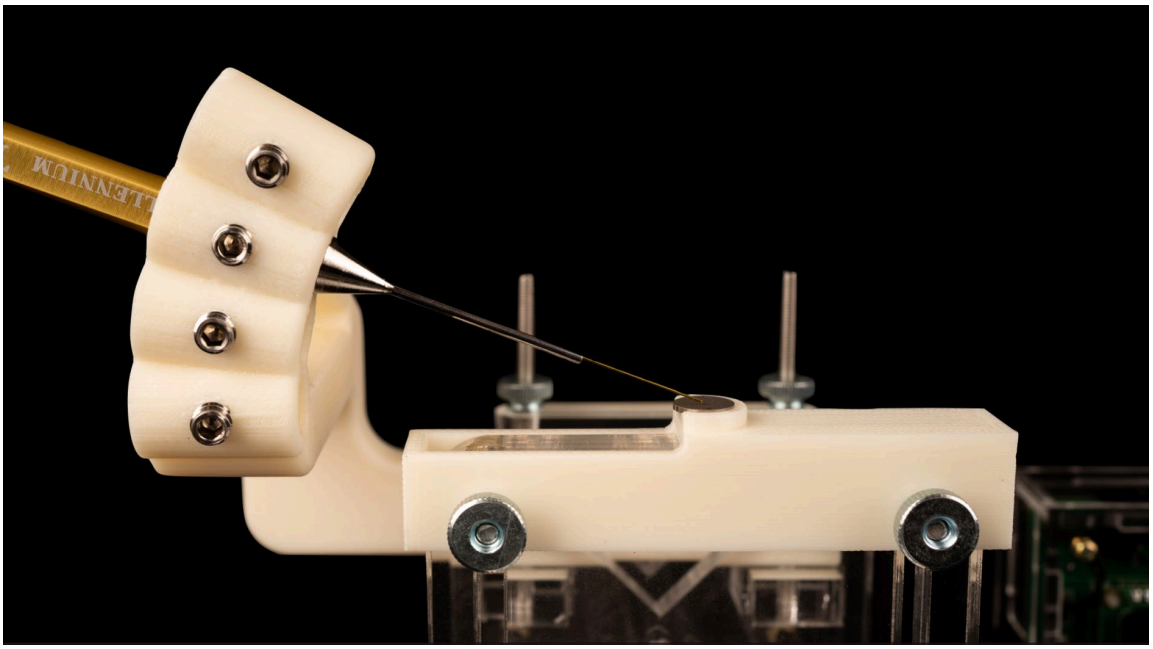

Figure 2. Custom jig assembly. Custom jig assembly with the laser handpiece and fiber in position relative to the titanium disk. Four openings in the assembly served as guide tubes, corresponding to the desired fiber-disk relationship angles being tested (0°, 10°, 20° and 30°). The jig assembly was affixed to the top of a programmable linear actuator. This image depicts the angulation of 20 degrees.

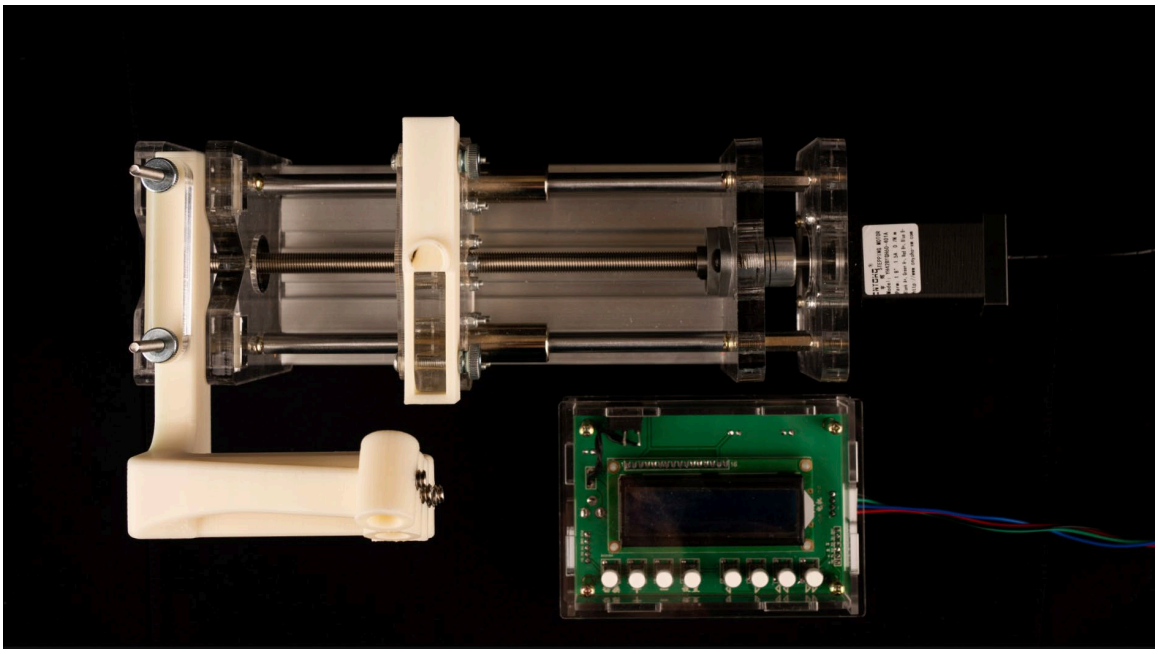

Figure 3. Programmable linear actuator. The linear actuator selected for this study (CYNOHO®) uses a powered motor to move an attached base component along a fixed track. A programmable device is connected to the actuator that allows for a set speed and time to run providing standardized energy delivery at a consistent angular orientation and repeatable speed.

CHAPTER 3: Results

Disk Exposure and Analysis Methodology

The custom jig assembly affixed to the programmable linear actuator proved to be a successful means to carry out the study. A controlled amount of energy was delivered to test disks in a standardized fashion. This protocol proved to be a consistent and repeatable method to mimic clinical treatment of peri-implantitis with an Nd:YAG laser approach. In terms of image capture, the laser scanning confocal microscope provided a sufficient mechanism to assess titanium surface characteristics.

Visual Appearance

When comparing the test groups, it is clear that there is a positive correlation between visual changes and increasing exposure angle (Figure 4). The unexposed areas of the disks and the 0° test group shows no differences. The 10° test group begins to show a faint gray color change in the irradiated areas that increased in darkness and clarity moving to 20° and then a dark, well-defined line is demonstrated in the 30° group. While exposing the disks at the steepest angle, smoke was observed to be coming off the surface of the disks with a noticeable increase in disk temperature.

Surface Topography Analysis

The FIJI software allows for a myriad of functions to observe and analyze the z-stack files. One way to view this data is in a 2-dimensional graph across the imaged

surfaces in what is termed a plot profile (Figure 5). This is demonstrated by assigning a gray value to each individual 3-dimensional pixel (voxel) compiled from the CZI files. The highest peaks are assigned a bright white-gray value while the lowest valleys are assigned a dark black-gray value. Another way to view this data is through the surface plot function (Figure 6), which provides a 3-dimensional representation of surface characteristics. Computed topography data was determined utilizing the SurfTool 1B and SurfCharJ 1q plugins (Figure 7). Ra was analyzed for all test disks and control areas. The mean Ra values were found to be similar across all groups, ranging from 3.10 μm in the control group and 3.51 μm in the 20° group. The standard deviation was lowest in the 10° group at 0.267 μm, and highest in the 20° group at 1.137 μm. Descriptive statistics and independent t-test analysis (Table 1) revealed no statistically significant changes in mean Ra values comparing any of the test groups to the control group, with the p-values ranging from 0.131 (20° group) to 0.400 (30° group). The hypothesis that the increase in laser angle would result in a decrease in surface roughness was tested using a one-way ANOVA (Table 2). It was found that there was not a statistically significant correlation for Ra, as the p-value was found to be 0.623. Based on the p-values above, the association that the titanium surface roughness decreases, as the laser angle increases has not been established at the 0.05 level of significance.

SURFACE ROUGHNESS PARAMETERS

Two additional surface roughness parameters were analyzed, Rt and Rq. Rt is defined as the difference between height of the highest peak and depth of the deepest valley within the evaluation length. Rq is the quadratic average, or root mean square

average of profile height deviations from the mean line. Following analysis of these additional parameters, the one-way ANOVA revealed similar results to that of Ra in that no significant surface roughness alterations were found as laser angle increased. However, when analyzing Rt, three of the test groups compared to controls were found to be statistically significant. Interestingly, the groups shown to be significant were the 0°, 10°, 20°, but not the 30°. The Rq data showed no statistically significant differences for all test groups compared to controls for the t-test comparison. Furthermore, no significant alterations were found using the one-way ANOVA, which was similar to findings in the other parameters evaluated.

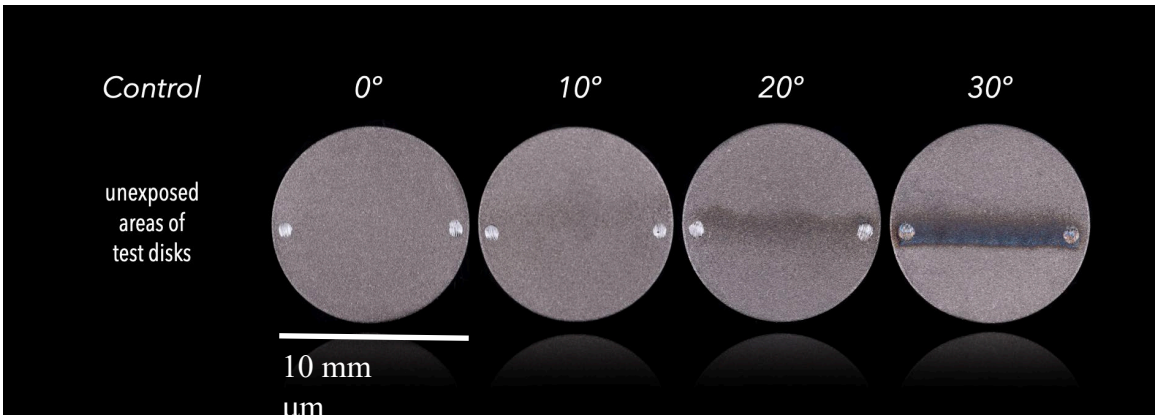

Figure 4. Photographs of sample disks. A positive correlation between visual changes and increasing exposure angle is shown in the photographic images. The unexposed areas of the disks and the 0° test group show no differences. The 10° test group begins to show a faint gray color change in the irradiated areas that increased in darkness and clarity moving to 20° and then a dark, well-defined line is demonstrated in the 30° group.

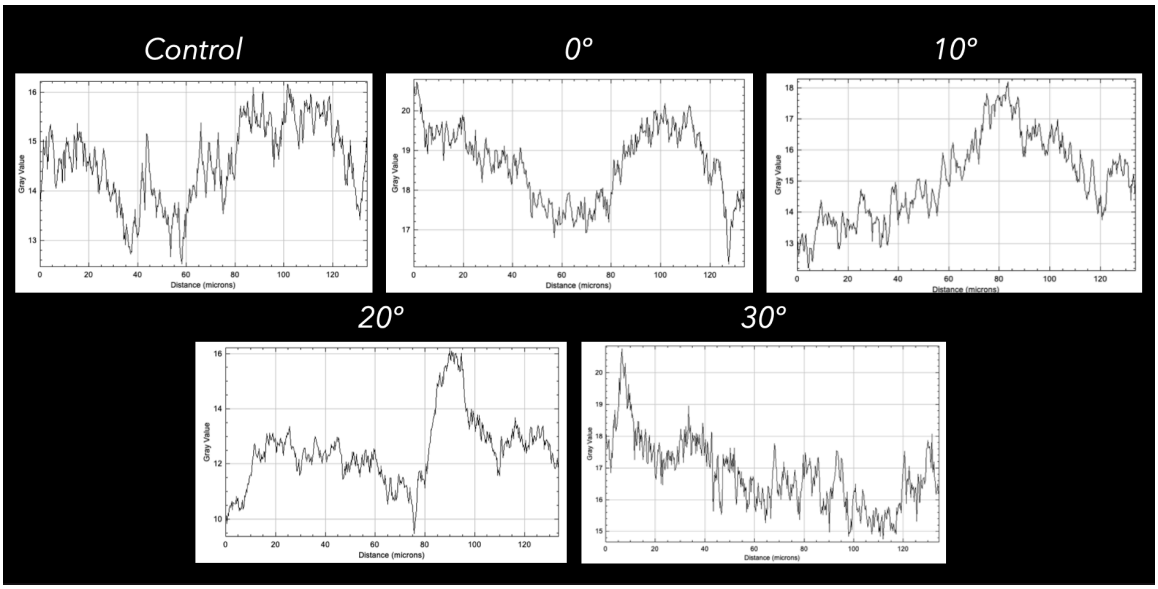

Figure 5. Plot profile images of the sample disks. Surface roughness is represented by assigned gray values corresponding to peaks and valleys across the distance measured. This is demonstrated by assigning a gray value to each individual 3-dimensional pixel (voxel) compiled from the CZI files. The highest peaks are assigned a bright white-gray value while the lowest valleys are assigned a dark black-gray value.

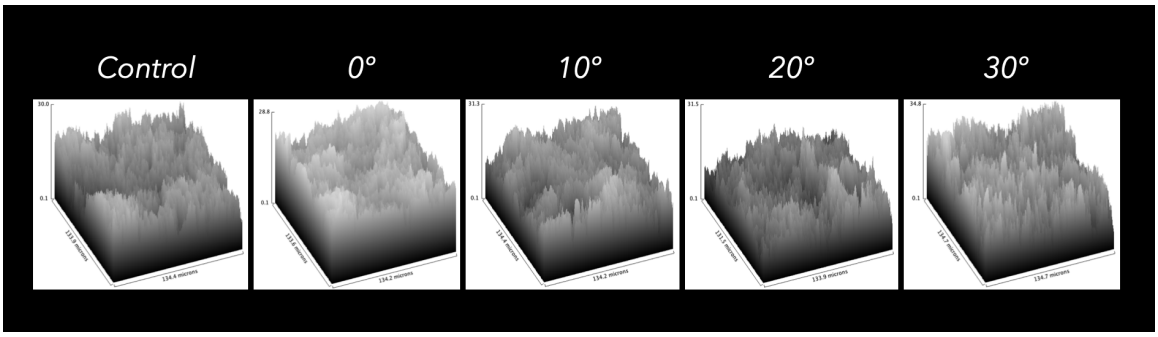

Figure 6. Surface plot images. Depicted are surface plot images of all sample test groups compared to controls, a 3-dimensional representation of surface roughness based on assigned gray values for the z-dimension. No statistically significant differences were noted between the controls and any of the test groups.

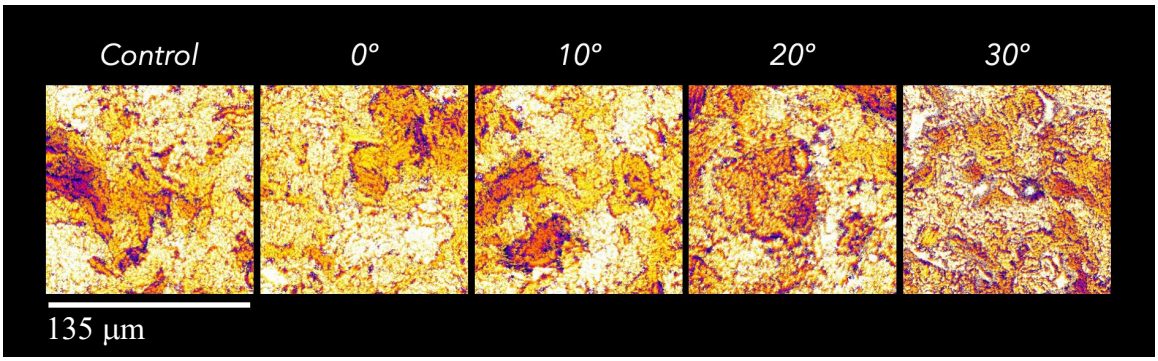

Figure 7. Computed topography images of sample disks. Computed topography data was determined utilizing the SurfTool 1B and SurfCharJ 1q plugins, which use complex algorithms to quantify data. Ra was analyzed for all test disks and control areas. The mean Ra values were found to be similar across all groups, ranging from 3.10 µm in the control group and 3.51 µm in the 20° group. The standard deviation was lowest in the 10° group at 0.267 µm, and highest in the 20° group at 1.137 µm.

Table 1. Descriptive Statistics and Independent t-test Analyzing Surface Roughness Parameters of Titanium Disk Groups

An asterisk indicates that there are significant differences in the mean roughness between a laser angle and the control as seen at the different property considerations. It can be seen that statistical significance was not established between the control and the 30° angle at Rt (difference between height of the highest peak and depth of the deepest valley within the evaluation length) property, nor any other groups when analyzing the Ra (arithmetic average of profile height deviations from the mean line) and Rq (quadratic average, or root mean square average of profile height deviations from the mean line) parameters.

Property	Group	Mean (N = 10) (μm)	STD Deviation (μm)	P-value
Ra	Control	3.10	0.644	--
	0 degree	3.48	0.407	0.137
	10 degree	3.47	0.267	0.122
	20 degree	3.51	0.481	0 .131
	30 degree	3.46	1.137	0.400
Rq	Control	3.82	0.776	--
	0 degree	4.34	0.451	0.093
	10 degree	4.32	0.325	0.087
	20 degree	4.35	0.533	0.097
	30 degree	4.25	1.325	0.392
Rt	Control	16.47	1.954	--
	0 degree	19.00	2.160	0.013*
	10 degree	18.69	1.592	0.012*
	20 degree	19.51	2.965	0.016*
	30 degree	18.51	2.800	0.077

Table 2. One-way ANOVA and Surface Roughness Parameters

The hypothesis proposed was that there would be a positive correlation with a decrease of mean surface roughness as laser angle increased. The above hypothesis was tested using a one-way ANOVA at each of the properties shown below.

Property	p-value
Ra	0.623
Rq	0.509
Rt	0.060

CHAPTER 4: Discussion

COMPARATIVE LITERATURE OUTCOMES

Previously completed studies have demonstrated titanium surface melting, cracking, and altered porosity following exposure with an Nd:YAG laser.[19] One publication by Romanos evaluated titanium disks that were roughened by three different methods including sandblasting, titanium plasma-spraying, and hydroxyapatite coating. They reported extensive melting in all irradiated areas of the titanium disks, which were observed with high-resolution scanning electron microscopy up to 1:20,000. Treated areas were described as having a relatively smooth surface; however, no quantitative data was gathered looking at surface roughness parameters. This study also evaluated the impact of diode laser treatment and found no modification of the disk surfaces even at the highest power setting.[19] Another study evaluating the effects of the Er,CR:YSGG showed melting and flattening of titanium disk surfaces at higher energy settings.[18] At lower energy settings, no observable changes were appreciated. Again, the results were obtained from visual inspection of scanning electron microscopy with no quantitative data reported. Important aspects to consider in these studies are the angle of energy exposure and variable orientations to the disk surface. The Romanos study describes the position of the laser fiber perpendicular to the disks, non-standardized linear movement, and various laser energy settings. Similarly, Ercan oriented the fiber perpendicular to the disks, but did not attempt to mimic clinical treatment as no movement was performed. Another study by Shin did quantify Ra values of irradiated areas using an Er:YAG laser.[22] These results showed a significant decrease in Ra comparing unexposed and exposed areas, but the study description provides no mention of fiber angulation.

The current study aimed to evaluate the effects of Nd:YAG laser exposure at clinically relevant angulations and energy values. The materials and methods conducted in this study provided for controlled orientation of the laser fiber, movement to simulate clinical treatment, and a standardized energy delivery. Furthermore, the image capture and analysis techniques used in the study allowed for observation of quantitative surface roughness parameters. As described above, no significant differences were found in terms of Ra comparing the unexposed areas to any of the angulations tested (0°, 10°, 20°, 30°).

Utilizing Ra values to quantify surface roughness is a common approach and is used historically across various industries. However, there are some inherent limitations in using this parameter as it does not differentiate between peaks and valleys. In contrast, Ra provides topographical information through calculated deviations from a determined mean line horizontally through a surface. Thus, additional parameters were also measured, including Rq and Rt. Neither of these parameters showed statistically significant differences regarding a correlation between decreased surface roughness with increases in exposure angulation. A significant difference was found when comparing control group Rt values and the 0°, 10°, 20° groups, but not the 30°. A possible explanation of this finding is the large standard deviation values shown in the 30° group. Surface roughness alterations may be occurring but the damage may not be in a uniform manner and is not well represented by the parameters analyzed. Sz is one surface roughness parameter that evaluates the difference between the highest and lowest points on a surface. In preliminary testing using a surface profiling machine, Sz was shown to have a significant level of variance amongst a small set of sample disks analyzed. Further

imaging and analysis using these methods may prove to yield statistically significant results compared to those demonstrated in the current study.

POTENTIAL CLINICAL IMPACT

Although significant surface roughness alterations were not demonstrated, this study shows a clear visual change to titanium surfaces exposed to Nd:YAG irradiation. This visual alteration intensified with increasing laser angulation, with the 30° group showing a stark delineation from unexposed to exposed areas. A possible explanation of this appearance relates to potential damage or alteration of the titanium oxide layer that exists along dental implant surfaces. This native oxide layer has been altered by dental implant manufacturers to increase beneficial biochemical interactions through enhanced cell attachment.[23] By achieving a thin and uniform titanium oxide layer, enhanced wettability has been reported that could aid in favorable interplay between host cells, tissues, and the implant surface.[24] Importantly, the characteristics of the titanium oxide layer can play a role in the osseointegration process required for successful dental implant integration and healing.[25] If this layer were to be damaged during peri-implant laser therapy, it could have a negative impact on how surrounding host cells and tissues interact with the titanium implant surface. Future studies evaluating the effects laser irradiation may have on the titanium oxide layer are warranted. Furthermore, biological implications could be further tested regarding possible alterations of the interactions between host cells and tissues and the titanium surface exposed to laser energy.

Another consideration to be discussed is the influence that implant crown contours have on laser angulation during treatment. As discussed earlier, in order to

achieve “ideal” angulation of the laser fiber, dental implant crowns should be removed prior to treatment. Crown contours vary based on a number of factors. Implant platform position is a significant influence on final implant crown contours as restorative providers fabricate restorations to align with adjacent dentition. Implant platform dimensions also play a role, as smaller diameter implants may require overcontoured restorations to fill large edentulous spaces. Furthermore, adjacent tooth anatomy impacts implant crown dimensions and can limit accessibility to implants for therapy. Peri-implant laser angulation is further complicated due to the subgingival nature of peri-implantitis. As discussed earlier, in order to achieve “ideal” angulation of the laser fiber, dental implant crowns require removal prior to treatment (Figure 1). Crown removal will improve fiber orientation and may prevent potential negative consequences of titanium surface irradiation.

CHAPTER 5: Conclusions

The custom jig and actuator assembly proved to be a reproducible method for standardized laser energy delivery. Confocal microscopy provided excellent imaging for quantification of surface topography characteristics. A one-way ANOVA revealed no significant differences in surface roughness (Ra) when comparing unexposed control areas to laser exposed areas at all angles tested. Therefore, the conclusion of this study is that there were no significant surface roughness alterations found on titanium implant disks following Nd:YAG laser irradiation up to an energy angulation of 30°. Future studies are needed to evaluate the potential biological implications irradiation angle may have when treating peri-implant conditions.

REFERENCES

1. Schwarz F, Derks J, Monje A, Wang H-L. Peri-implantitis. *Journal of Periodontology*. 2018;89.

2. Heitz-Mayfield LJA, Salvi GE. Peri-implant mucositis. *Journal of Periodontology*. 2018;89. doi:10.1002/jper.16-0488.

3. Elani HW, Starr JR, Da Silva JD, Gallucci GO. Trends in dental implant use in the U.S., 1999–2016, and projections to 2026. *Journal of Dental Research*. 2018;97(13):1424-1430.

4. Derks J, Tomasi C. Peri-implant health and disease. A systematic review of current epidemiology. *Journal of Clinical Periodontology*. 2015;42.

5. Roccuzzo M, Mirra D, Pittoni D, Ramieri G, Roccuzzo A. Reconstructive treatment of Peri-implantitis infrabony defects of various configurations: 5-year survival and success. *Clinical Oral Implants Research*. 2021;32(10):1209-1217.

6. Schwarz F, John G, Mainusch S, Sahm N, Becker J. Combined surgical therapy of peri-implantitis evaluating two methods of surface debridement and decontamination. A two-year clinical follow up report. *Journal of Clinical Periodontology*. 2012;39(8):789-797.

7. Coluzzi, D. Fundamentals of lasers in dentistry: basic science, tissue interaction, and instrumentation. *Journal of Laser Dentistry*. 2008;16(Spec. Issue): 4-10.

8. Myers TD, Myers WD. The use of a laser for debridement of incipient caries. *The Journal of Prosthetic Dentistry*. 1985;53(6):776-779.

9. Schwarz F, Nuesry E, Bieling K, Herten M, Becker J. Influence of an erbium, chromium-doped yttrium, scandium, gallium, and garnet (ER,CR:YSGG) laser on the reestablishment of the biocompatibility of contaminated titanium implant surfaces. *Journal of Periodontology*. 2006;77(11):1820-1827.

10. Nevins M, Kim S-W, Camelo M, Sanz Martin I, Kim D, Nevins M. A prospective 9-month human clinical evaluation of laser-assisted new attachment procedure (LANAP) therapy. *The International Journal of Periodontics & Restorative Dentistry*. 2014;34(1):21-27.

11. Wigdor HA, Walsh JT, Featherstone JD, Visuri SR, Fried D, Waldvogel JL. Lasers in Dentistry. *Lasers in Surgery and Medicine*. 1995;16(2):103-133.

12. Bader HI. Use of lasers in Periodontics. *Dental Clinics of North America*. 2000;44(4):779-791.

13. Mills MP, Rosen PS, Chambrone L, et al. American Academy of Periodontology Best Evidence Consensus Statement on the efficacy of laser therapy used alone or as an adjunct to non-surgical and surgical treatment of periodontitis and peri-implant diseases. *Journal of Periodontology*. 2018;89(7):737-742.

14. Kilinc E, Rothrock J, Migliorati E. Potential surface alteration effects of laser-assisted periodontal surgery on existing dental restorations. *Quintessence Int.* 2012 May;43(5):387-95.

15. Raghavendra S, Wood MC, Taylor TD. Early wound healing around endosseous implants: a review of the literature. *International Journal of Oral Maxillofacial Implants.* May-Jun 2005;20(3):425-31.

16. Albrektsson T, Wennerberg A. Oral implant surfaces: Part 2--review focusing on clinical knowledge of different surfaces**.** *International Journal of Prosthodontics*. Sep-Oct 2004;17(5):544-64.

17. Schwarz F, Aoki A, Sculean A, Becker J. The impact of laser application on periodontal and peri-implant wound healing. *Periodontology 2000*. 2009;51(1):79-108.

18. Ercan E, Candirli C, Arin T, Kara L, Uysal C. The effect of ER,CR:YSGG laser irradiation on titanium discs with microtextured surface morphology. *Lasers in Medical Science*. 2013;30(1):11-15.

19. Romanos GE, Everts H, Nentwig GH. Effects of diode and nd:YAG laser irradiation on titanium discs: A scanning electron microscope examination. *Journal of Periodontology*. 2000;71(5):810-815.

20. Burgueño-Barris G, Camps-Font O, Figueiredo R, Valmaseda-Castellón E. The influence of implantoplasty on surface roughness, biofilm formation, and biocompatibility of Titanium Implants: A systematic review. *The International Journal of Oral & Maxillofacial Implants*. 2021;36(5).

21. Chinga G, Johnsen P, Dougherty R. Quantification of the 3D microstructure of SC surfaces. *Journal of Microscopy*. 2007;227(3):254-265.

22. Shin S-I, Min H-K, Park B-H, et al. The effect of ER:YAG laser irradiation on the scanning electron microscopic structure and surface roughness of various implant surfaces: An in vitro study. *Lasers in Medical Science*. 2010;26(6):767-776.

23. Ekoi EJ, Stallard C, Reid I, Dowling DP. Tailoring oxide-layer formation on titanium substrates using microwave plasma treatments. *Surface and Coatings Technology*. 2017;325:299-307.

24. Luo X, Zhu Z, Tian Y, You J, Jiang L. Titanium dioxide derived materials with Superwettability. *Catalysts*. 2021;11(4):425.

25. Jasinski JJ. Hybrid oxidation of titanium substrates for biomedical applications. *2nd Coatings and Interfaces Web Conference (CIWC-2 2020)*. 2020.